Data in Brief 21 (2018) 1954–1962

Contents lists available at ScienceDirect

Data in Brief

journal homepage: www.elsevier.com/locate/dib

Data Article

A dataset of the study on design parameters for the solar photovoltaic charge controller

M. Premkumar [a,*], R. Sowmya [b], K. Karthick [a]

[a] GMR Institute of Technology, India
[b] National Institute of Technology, India

ARTICLE INFO

Article history:
Received 29 September 2018
Received in revised form
26 October 2018
Accepted 13 November 2018
Available online 16 November 2018

ABSTRACT

This set of data is being used to calculate the design parameters of the solar photovoltaic (PV) charge controller. The data presented in this paper are used to design an advanced charge control with higher capacity and more possible real-time applications. This design parameters of the controller will be useful for the off-grid systems, automatic street light, and signs control, etc., which requires the medium-level power, and more reliable operation. The design set of parameters such as inductance, switching frequency, duty cycle, power loss, and the efficiency are given in this paper for the rating of the 500 W charge controller. The data captured are compared with the various power level selection along with the different power semiconductor switches.

Specifications table

Subject area	*Renewable Energy.*
More specific subject area	*Battery Charge Controller.*
Type of data	*Table, Graph, and figures.*
How data was acquired	*Experimental setup of solar PV based battery charge controller using the sensors such as a current sensor, voltage sensor along with the data acquisition system.*

* Corresponding author.
E-mail address: premkumar.m@gmrit.org (M. Premkumar).

https://doi.org/10.1016/j.dib.2018.11.064

Data format	*Raw, Calculated, Analyzed, Tabulated, and Plotted.*
Experimental factors	*Normalized data considered from the manufacturer's datasheet as per the requirements.*
Experimental features	*The solar-based charge controller is tested with the different power switches and various levels of load power range for the performance analysis of the charge controller.*
Data source location	*Power Electronics Laboratory, GMR Institute of Technology, Rajam, Srikakulam, Andhra Pradesh, India.*
Data accessibility	*The performance study data are included in this paper.*

Value of the data

- The first highlight of this set of data on MPPT battery charge controller is to understand the selection of the proper power semiconductor switch for the required power level.
- The dataset presented in this paper helps and enables the researchers in the field of battery charge controller for the roof-top PV energy generation at off-grid, street light controllers, and urban homes.
- The dataset enables to verify the voltage rating of the components and checks the compatibility of the buck converter capacitors, inductors and pulse-width-modulation (PWM) algorithm during the charge controller operation.
- This dataset enables the designers to design a better controller with higher efficiency and helps to find the optimal operation of the controller at the required power level.

1. Data

The design and implementation of the charge controller start essentially with the buck converter design which consisting of the power switching device (MOSFET), capacitor, and an inductor with 40 A current rating. The multiple units will be combined into the final controller to reach the target rating. The essential requirement in designing the charge controller is efficiency, and the initial design at 96% efficiency with 4% power losses. At 40 A rating with a 12 V battery, the power loss is equated to 20 W. The heat generation due to this power loss does not require any forced cooling. The metal heat sinks for the main components, and consistent airflow should be provided through the enclosure [1]. The specification details of the charge controller are given in Table 1.

The dataset presented in this paper is grouped into two parts: (i) Sizing of an inductor, design and the impact on the efficiency; (2) selection of the switching element (MOSFET), and the impact on the efficiency. With one-stage output at the light-load condition, the buck converter should operate at the discontinuous current mode (DCM). After the careful analysis, the converter delivers a higher efficiency during DCM with one diode for the ground route, compared with the synchronous converter using MOSFET at the ground path [2,3]. The efficiency at high load is less due to the diode in the ground path of the asynchronous buck converter. To increase the efficiency, the MOSFET is connected in the ground path of the asynchronous buck converter called as modular design presented in this paper. The schematic diagram of the charge controller is shown in Fig. 1.

Table 1
Controller specification details.

Controller parameters	Values
Solar PV Panel Voltage (V)	30
Battery Voltage (V)	12.5
Output Current (A)	40
Output Power (W)	500

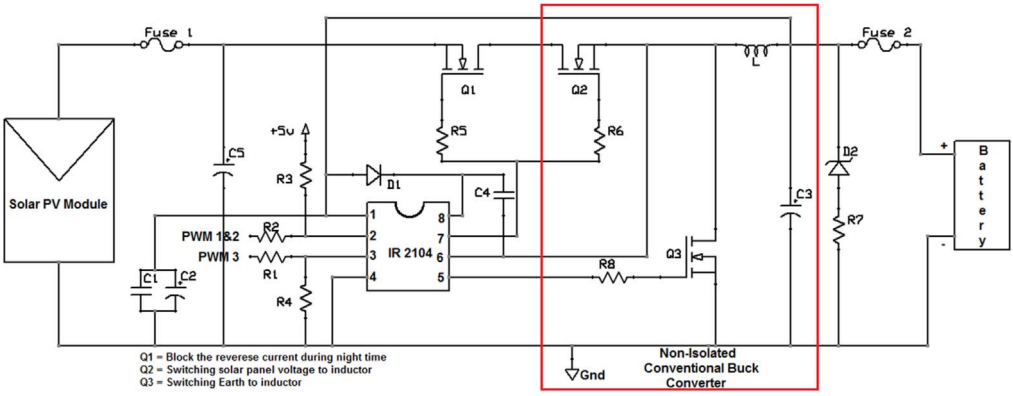

Fig. 1. Modular design of the asynchronous buck converter as solar charge controller.

Table 2
Converter design using surface mount switch.

MOSFET	**CSD19502Q5B**					
Panel voltage (V)	18	30	60	30	60	60
Battery voltage (V)	12.5			25		50
Load current (%)	**Efficiency**					
1	−6.03%	−8.04%	−80.96%	46.79%	−96.52%	67.58%
5	78.74%	78.34%	63.76%	89.33%	60.67%	93.50%
10	89.27%	89.10%	81.82%	94.61%	80.30%	96.73%
20	94.45%	94.37%	90.77%	97.21%	90.07%	98.31%
50	97.31%	97.30%	95.91%	98.65%	95.79%	99.20%
80	97.78%	97.82%	97.04%	98.89%	97.10%	99.36%
100	97.84%	97.89%	97.34%	98.92%	97.49%	99.39%

The efficiency calculation results for first-pass asynchronous converter design at all power levels. The design dataset with different power switches (after careful comparison among 15 switching MOSFETs) for the various PV panel voltage is presented in Tables 2–3. Tables 2–3 help the designers to select the optimal switch for the charge controller design.

In Tables 2–3, the negative efficiency indicates that the total power loss of the charge controller is more than the total output power under 1% of the load current due to the contribution of the inductor core loss. The initial tentative efficiency assumption is 96%, this needs to be split into the different components. The 4% losses to be allocated as follows:

- 0.9% AC loss at 40 A inductor current
- 0.9% DC loss at 40 A inductor current
- 0.8% loss due to switching devices
- 0.6% loss due to the capacitor
- 0.8% loss due to the microcontroller and miscellaneous

2. Experimental design, materials, and methods

2.1. The dataset for inductor design

The required inductance to allow the continuous current flow to the load is a key point in inductor design. The inductor should have low resistance to maintain the power loss within the limit. The dc

Table 3
Converter design using TO220 through-hole switch.

MOSFET	PSMN3R3-80PS			FDP150N10A		
Panel voltage (V)	18	30	60	30	60	60
Battery voltage (V)	12.5			25		50
Load current (%)	**Efficiency**					
1	69.59%	−8.21%	−128.73%	82.10%	−127.07%	64.30%
5	93.90%	78.36%	54.33%	96.42%	54.62%	92.87%
10	96.84%	89.14%	77.17%	98.16%	77.31%	96.43%
20	98.22%	94.38%	88.46%	98.97%	88.61%	98.16%
50	98.80%	97.27%	94.93%	99.33%	95.18%	99.12%
80	98.70%	97.78%	96.39%	99.31%	96.71%	99.30%
100	98.56%	97.85%	96.80%	99.25%	97.17%	99.34%

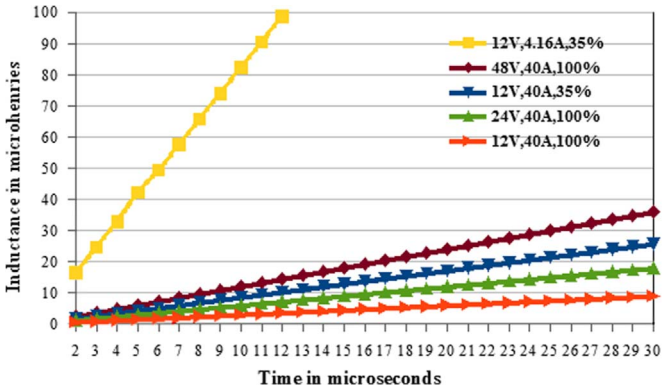

Fig. 2. Inductor size requirements (% indicates the percentage of average DC).

voltage drop across the inductor is 0.108 V for the assumption of 0.9% DC loss. The series resistance for the inductor of 40 A rating is around 2.4 mΩ. The value of the inductance depends on the switching frequency. The inductance is required to keep the current flow only to the battery when the PV panel switch is OFF, and earth switch is ON. The relation between the inductance requirement and the earth ON time for the various battery operating voltage is shown in Fig. 1, and this chart will be helpful for the designers to select the inductance value for the different rating of the battery. The time axis in Fig. 2 interpreted for the switching frequency of 50 kHz, and a PWM (i.e., ratio between the battery voltage to the PV panel output voltage) of 50%, a total switching time of 20 μs and earth ON time of 10 μs.

The switching timing for the Earth switch and PV panel switch are listed in Tables 4–5 for 10 μH as an arbitrary, and these values are applicable for a 100% ripple factor, but it is too high to ensure the operation, mainly when the battery is under boost charging with a higher voltage. The maximum Earth ON time is reduced under a boost charging as shown in Table 5. For the better operation, the switching time is to be followed as per the data from the Table 5.

The Tables 4–5 shows the minimum switching frequency for the converter with 10 μH inductance and 100% ripple current. In practice, the ripple factor will be reduced by increasing the switching frequency. However, the losses will be reduced by the selecting the lower switching frequency. When the researchers focus on the charging the battery with boost mode, Table 5 helps to select the switching frequency. So, the frequency limit for the converter switching is presented in Fig. 3. The summary of the dataset for inductor design is listed in Table 6.

Table 6 gives the overall design data for the solar based charge controller. From the summary, the dual T-130-26 core gave the best result and used as a single inductor. For 500 W design, AWG #12

Table 4
PWM ratio and switching frequency requirement for 10 μH inductance.

PWM and timing table for normal charging			The timing for 10 μH		
PV voltage (V)	**Battery voltage (V)**	**PWM ratio**	**Earth ON (μs)**	**Panel ON (μs)**	**Frequency (Hz)**
18	12	0.667	33	99	7,576
30	12	0.4	33	55	11,364
60	12	0.2	33	41.25	13,468
30	24	0.8	16	80	10,417
60	24	0.4	16	26.667	23,438
60	48	0.8	8	40	20,833

Table 5
PWM ratio and switching frequency requirement for 10 μH inductance with boost charging.

PWM and timing table for boost charging			The timing for 10 μH		
PV voltage (V)	**Battery voltage (V)**	**PWM ratio**	**Earth ON (μs)**	**Panel ON (μs)**	**Frequency (Hz)**
18	16	0.889	28	252	3,571
30	16	0.533	28	60	11,364
60	16	0.267	28	38.18	15,110
30	29.9	0.997	14	4200	237
60	32	0.533	14	30	22,727
60	59.9	0.998	6	3600	277

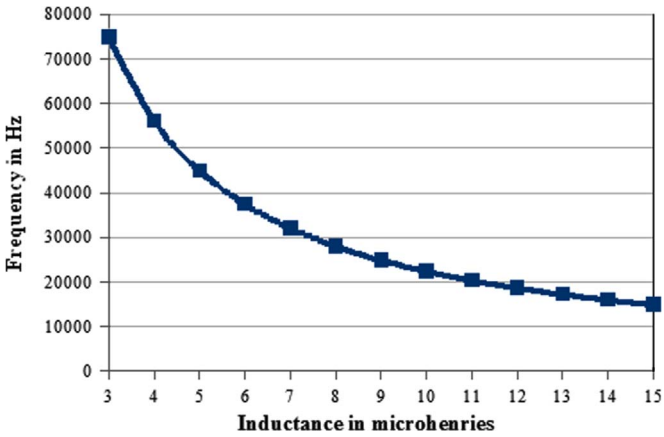

Fig. 3. The requirement of the minimum switching frequency.

wire of four strands are twisted and wound on the pair of cores may be useful. It results in an inductance of 15.7 μH, and the ripple current of 23% at full load with 50 kHz switching frequency. The power loss is 2 W, and the design uses 3.3 m of AWG #12 lacquered wire. The four strands of the conductor should have the same twist so that the conductor has the equal length adjacent to the inner part of the core. This section of the paper has given enough dataset for the designers to select the proper value of inductor concerning the switching frequency, power loss, and rating of the charge controller.

Table 6
Selection of the proper inductor for 500 W charge controller.

Summary table Type of the Inductor	Trial 1 2 Inductors T106+multi wire	Trial 2 2 Cores 1 inductor T106+multi wire	Trial 3 1 Core T130+multi wire	Trial 4 2 Cores 1 inductor T130+multi wire	Trial 5 1 Core T157+multi wire
Input voltage	30	30	30	30	30
Output voltage	12.5	12.5	12.5	12.5	12.5
Input power	500	500	500	500	500
Output current (DC average)	40	40	40	40	40
Frequency	50,000	50,000	50,000	50,000	50,000
Duty cycle	0.417	0.417	0.417	0.417	0.417
Ripple current vs. Load current	36%	36%	36%	36%	36%
Ripple current (absolute, p-p)	14.4	14.4	14.4	14.4	14.4
Inductor value (Microhenry)	10.13	10.13	10.13	10.13	10.13
Max. current	47.2	47.2	47.2	47.2	47.2
Min. current	32.8	32.8	32.8	32.8	32.8
Core dimensions (mm)/Type code	T-106-26	T-106-26	T-130-26	T-130-26	T-157-26
OD	26.924	26.924	33.02	33.02	39.878
ID	14.478	14.478	19.812	19.812	24.13
Width	11.10	22.20	11.10	22.20	14.48
AI (μH/100 turns)	900	1800	785	1570	970
Turns for required inductance	10.61	7.50	11.36	8.03	10.22
Actual turns	16	10	12	10	12
Actual composite inductance	11.52	18	11.304	15.7	13.968
Total length (wire making bundles) (m)	3.22	3.11	2.65	3.28	3.27
Inductor DC resistance milliohms	1.33	1.61	1.37	1.07	1.07
DC Voltage drop in inductor (V)	0.05	0.06	0.05	0.04	0.04
Power in DC resistive loss (Watts)	2.12	2.57	2.20	1.71	1.70
Skin depth in copper	0.30	0.30	0.30	0.30	0.30
Wire diameter/skin depth	4.36	5.50	5.50	6.93	6.93
R_{ac}/R_{dc} (from micrometals graph)	3.00	3.00	3.00	3.00	3.00
R_{ac} (milliohms)	3.98	4.83	4.12	3.21	3.20
AC voltage drop in inductor	0.01	0.01	0.02	0.01	0.01
Power in AC resistive loss (Watts)	0.05	0.03	0.06	0.02	0.03
Total resistive power loss in inductor	2.17	2.60	2.25	1.73	1.73
Flux density B_{max}	164.94	131.95	207.24	124.34	133.25
Calculated core loss for given flux	40.47	25.72	64.34	22.80	26.24
Volume of core (cm^3)	8.98	8.98	6.08	12.17	11.46
Core loss (W)	0.54	0.23	0.49	0.28	0.92
Total power loss in inductor	2.71	2.83	2.74	2.01	2.65
Percent of rating used	92%	96%	136%	50%	88%

2.2. The dataset for selecting the MOSFET switch and its impact on the efficiency

Depends upon the voltage rating of the converter, the switch has to be selected. The converter in this paper requires 80 V on the average because the switches from Q1-Q3 requires a minimum voltage rating of 80 V. The critical factors in selecting the proper switch are based on on-state resistance, and rise time and fall time when ON and OFF period of the switch. Few switches require body diode or an additional diode across the switch [1–3]. The switch Q2 has to change between PV panel voltage and Earth, so it exhibits power pulsation during switch ON/OFF condition. The switch Q3 is protected by the body diode and is switching between the body diode forward voltage and Earth. So, it creates less power pulsation. Since the switch Q1 is switch ON/OFF rarely, the rise and fall time are immaterial. By keeping these factors in mind, there are 10 MOSFET versions with 2.8 mΩ–21 mΩ and the sum of rising and fall time from 12 ns–874 ns for the 500 W charge controller. The designers can consider any of the following MOSFETs for the design. The switches are: AP9970GP, CSD19502Q5B, FDP100N10A,

Table 7
Dataset for selecting the optimal MOSFET switch for 500 W controller.

MOSFET type	CSD1950	PSMN3	FDP150	IRFB	NTMFS	IXTK250	FDP100	STP50	IXFH150	AP99	MTY100
	2Q5B	R3-80PS	N10A	4321	6B14N	N10	N10A	NE10	N17T	70GP	N10E
$R_{ds\text{-}ON}$ (mΩ)	3.4	2.8	12.5	15	12.2	5	10	21	12	3.2	11
V_{dss} (V)	80	100	100	150	100	100	100	100	175	60	100
I_d (A)	100	120	50	85	50	250	75	50	150	240	100
V_{gc} (pF)	4870	9961	1440	4460	1300	12700	7300	6000	9800	6430	10640
$T_{d\text{-}ON}$ (ns)	8	41	13	18	9.6	35	70	25	22	180	48
T_r (ns)	6	43	16	60	39	40	265	100	30	200	490
$T_{d\text{-}OFF}$ (ns)	22	109	21	25	17	120	125	45	58	180	186
T_f (ns)	7	44	5	35	6.8	55	115	35	30	240	384
V_{ds} (V)	0.8	1.2	1.3	0.8	1.2	1.2	1.25	1.5	1.2	1.3	1.2
Packaging	SON 5*6	TO220	TO220	TO220	488AA	TO264	TO220	TO220	TO247	TO220	TO264
Cost per unit (Approx.)	$8.69	$8.67	$5	$30	$3.14	$10.80	$8.75	$4.54	$10.41	$100.00	100
Vendor	Verical	Ameya	Verical	Verical	Digikey	Mouser		Solaluna88	Mouser	Comet	Mouser

Table 8
Cost data of the switches for the charge controller.

CSD19502Q5B				FDP150N10A				PSMN3R3-80PS			
Panel voltage (V)	**Battery voltage (V)**	**Switch power loss (%)**	**MOSFET cost for the controller ($)**	**Panel voltage (V)**	**Battery voltage (V)**	**Switch power loss (W)**	**MOSFET cost for the controller ($)**	**Panel voltage (V)**	**Battery voltage (V)**	**Switch power loss (W)**	**MOSFET cost for the controller ($)**
60	12.5	0.81	$22.03	60	12.5	0.79	$54.25	60	12.5	0.88	$57.07
30	12.5	0.79		30	12.5	0.74		30	12.5	1.47	
18	12.5	0.84		18	12.5	0.79		18	12.5	1.32	
30	25	0.45		30	25	0.44		30	25	0.78	
60	25	0.44		60	25	0.43		60	25	1	
60	50	0.45		60	50	0.25		60	50	0.52	

FDP150N10A, IRFB4321, IXTK250N10, IXFH150N17T, MTY100N10E, NTMFS6B14N, PSMN3R3-80PS, and STP50NE10.

For the switches Q1 and Q3, a low $R_{ds\text{-}on}$ is the main requirement, and the switch Q2 requires a low $R_{ds\text{-}on}$, low rise and fall time. Table 7 helps the designers to select the MOSFET switch for the 500 W charge controller application. Based on the factors such as on-state resistance, rise and fall time, and additional diodes, the researcher can pick the correct switch for their needs. The switch CSD1950Q5B is superior in both the low $R_{ds\text{-}on}$ and the timing. However, a surface mount design makes the design complexity for the designers. So, for the switch Q1 and Q3, PSMN3R3-80PS is preferred because the rise time and fall time is not a consideration. The switch Q2 prefers the FDP150N10A as per the requirements mentioned above. Table 8 discusses the cost analysis, and power loss contribution of the most preferred switch such as CSD19502Q5B, FDP150N10A, and PSMN3R3-80PS. These switches are preferred only for the rating of 500 W. The dataset presented in this paper is only for the charge controller with 30 V panel voltage, 12.5 V battery voltage, and 500 W output power. The performance of the preferred switch for this application is presented in Tables 2–3.

Acknowledgements

We extend our thankfulness to GMR Institute of Technology, Rajam for allowing us to validate the charge controller design data in the closed-environment at power electronics laboratory.

Transparency document. Supporting information

Transparency data associated with this article can be found in the online version at https://doi.org/10.1016/j.dib.2018.11.064.

References

[1] N. Khera, N. Rana, S. Narendiran, S.K. Sahoo and M. Balamurugan, Design of charge controller for solar PV systems, in: Proceedings of International Conference on Control, Instrumentation, Communication and Computational Technologies, India pp. 149–153, 2015.
[2] S.D. Gupta, Md AbidHasan, Md Sajid Hossain, S.M. Ariful Haque, S.T. Mowri, Design & implementation of an improved solar charge controller for variable range of solar panels, Am. J. Eng. Technol. Res. 14 (2) (2014) 65–74.
[3] M. Lokesh Reddy, P.J.R. Pavan Kumar, S. Aneel Manik Chandra, T. Sudhakar Babu, N. Rajasekar, Comparative study on charge controller techniques for solar PV system, Energy Procedia 117 (2017) 1070–1077.